Regulation of Microtubule Dynamics and Nucleation during Polarization in MDCK II Cells

M.-H. Bré,* R. Pepperkok, A. M. Hill,* N. Levilliers,* W. Ansorge, E. H. K. Stelzer, and E. Karsenti

European Molecular Biology Laboratory, D-6900 Heidelberg, Federal Republic of Germany and * Laboratoire de Biologie Cellulaire 4, U. A. Centre National de la Recherche Scientifique, 1134, Université Paris-Sud, 91405 Orsay-Cedex, France

Abstract. MDCK cells form a polarized epithelium when they reach confluence in tissue culture. We have previously shown that concomitantly with the establishment of intercellular junctions, centrioles separate and microtubules lose their radial organization (Bacallao, R., C. Antony, C. Dotti, E. Karsenti, E. H. K. Stelzer, and K. Simons. 1989. *J. Cell Biol.* 109:2817–2832. Buendia, B., M. H. Bré, G. Griffiths, and E. Karsenti. 1990. 110:1123–1136). In this work, we have examined the pattern of microtubule nucleation before and after the establishment of intercellular contacts. We analyzed the elongation rate and stability of microtubules in single and confluent cells. This was achieved by microinjection of *Paramecium* axonemal tubulin and detection of the newly incorporated subunits by an antibody directed specifically against the *Paramecium* axonemal tubulin. The determination of newly nucleated microtubule localization has been made possible by the use of advanced double-immunofluorescence confocal microscopy. We have shown that in single cells, newly nucleated microtubules originate from several sites concentrated in a region localized close to the nucleus and not from a single spot that could correspond to a pair of centrioles. In confluent cells, newly nucleated microtubules were still more dispersed. The microtubule elongation rate of individual microtubules was not different in single and confluent cells (4 μm/min). However, in confluent cells, the population of long lived microtubules was strongly increased. In single or subconfluent cells most microtubules showed a $t_{1/2}$ of <30 min, whereas in confluent monolayers, a large population of microtubules had a $t_{1/2}$ of >2 h. These results, together with previous observations cited above, indicate that during the establishment of polarity in MDCK cells, microtubule reorganization involves both a relocalization of microtubule-nucleating activity and increased microtubule stabilization.

THE complex three-dimensional organization of metazoa involves the differentiation, during embryogenesis, of organs fulfilling highly complex functions. This is reflected, at the cellular level, by a specific spatial organization of the cytoplasm. In the cells of each tissue, the relative positions of the nucleus, mitochondria, and Golgi apparatus are different. As far as cytoplasmic polarity and organization is concerned, microtubules are of special interest. Indeed, they are by essence unstable (Mitchison and Kirschner, 1984) and in equilibrium with a pool of soluble subunits in the cytoplasm (Inoué, 1981). They are polar and this polarity is what determines the positioning of the Golgi apparatus, for example (Bacallao et al., 1989; Kreis et al., 1988; Tassin et al., 1985*b*; Thyberg and Moskalewski, 1985; Vale, 1987). Therefore, to understand how the Golgi apparatus and other cytoplasmic organelles are positioned in different cells, it is essential to understand how microtubule polarity is oriented and to identify the signals controlling this orientation. Microtubule orientation could be determined by changing the position of the nucleating material relative to the nucleus or other cellular elements (minus end positioning, Baas et al., 1989; Bacallao et al., 1989; Buendia et al., 1990; Tassin et al., 1985*a*), as well as through specific stabilization of the microtubule plus end in local areas of the cytoplasm. This could be achieved either by capping the microtubule plus ends (Kirschner and Mitchison, 1986; Mogensen et al., 1989) or by the binding of microtubule-associated proteins (MAPs)[1] along the microtubule walls only in specific domains of the cytoplasm. In fact, a tight control of both microtubule nucleation and dynamics may be required to determine the precise orientation of microtubule networks during cell differentiation.

We are currently investigating the organization of microtubules during the establishment of polarity in epithelial cells (MDCK II cells). These cells form a polarized epithelium when they reach confluency in tissue culture (Balcarova-Stander et al., 1984). In isolated cells, microtubules originate from a broad region containing the centrioles. However, after the establishment of cellular junctions, the centrioles separate, and the microtubules lose their radial organization. Finally, in fully polarized cells, the microtubules are ar-

1. *Abbreviations used in this paper*: MAP, microtubule-associated protein; MCM, modular confocal microscope.

ranged along the apicobasal axis, with their plus end facing the basolateral domain, the centrioles being positioned just below the apical plasma membrane (Bacallao et al., 1989; Bré et al., 1987; Buendia et al., 1990). Interestingly, most microtubules do not originate directly from the centrioles or centriole proximity, suggesting that microtubule nucleation occurs either randomly in the cytoplasm because of the presence of soluble microtubule stabilizing factors or from nucleating material not strongly associated with the centrioles (Bré et al., 1987). In this work, we have investigated further the localization of newly nucleated microtubules in isolated cells and in confluent cells. This was done by microinjection of *Paramecium* axonemal tubulin, and detection of the newly incorporated subunits by an antibody directed against the *Paramecium* axonemal tubulin. Such an approach was first used successfully for analyzing microtubule nucleation and stability in PTK2 cells, especially during mitosis (Geuens et al., 1989). We also compared the microtubule elongation rate and stability in isolated and confluent cells. We found that when cells became fully surrounded by neighbors, the newly nucleated microtubules dispersed in the cytoplasm and microtubule stability increased. However, the microtubule elongation rate of individual microtubules was not substantially affected. These results suggest that nucleating material is relocalized after the establishment of cell contacts and that microtubules become progressively more stable. This latter point is further demonstrated quantitatively by Pepperkok et al. (1990).

Materials and Methods

Cells

MDCK II cells were grown in Eagle's MEM supplemented with 10 mM Hepes pH 7.3, 1% L-glutamine, 5% FCS, 110 U/ml penicillin, and 100 μg/ml streptomycin. African green monkey kidney (Vero) cells were grown as previously described (Kreis, 1986). The cells were seeded at appropriate dilutions on glass coverslips in order to get either individual, subconfluent or confluent cells after 18 h of incubation in a humidified atmosphere equilibrated with 5% CO_2 in air at 37°C.

Tubulin and Antitubulin Preparation

Paramecium axonemal tubulin and the specific, affinity-purified antibody against this tubulin were prepared as previously described (Adoutte et al., 1985; Cohen et al., 1982; Geuens et al., 1989).

Microinjection

Cells growing on glass coverslips marked with crossed lines were placed in a microinjection chamber in which the temperature was maintained at 37°C. The cells were immersed in 3 ml of culture medium and observed with an inverted microscope during microinjection. The cells were microinjected using an automated microinjection system (Carl Zeiss GmBH Oberkochen, FRG; Pepperkok et al., 1988). The *Paramecium* tubulin was diluted in a buffer containing 20 mM glutamate, 1 mM $MgCl_2$, 1 mM GTP, 1 mM EGTA, 1 mM DTT (pH 6.8). The microinjection was monitored and recorded on a videotape recorder (VTR NV 8030; National time lapse). The cells injected at a precise time were traced back on the video recording.

Detection of the Dynamic Network by Conventional Immunofluorescence Microscopy

After microinjection of the solution of *Paramecium* axonemal tubulin (1 mg/ml), the cells were washed for 2 s in PBS at 37°C, preextracted 10 s in microtubule-stabilizing buffer (80 mM K-Pipes pH 6.8, 5 mM EGTA, 1 mM $MgCl_2$, 0.5% Triton X-100) and fixed in methanol at −20°C for 5 min. This fixation procedure allows a good visualization of labeled segments and nucleation pattern in MDCK cells. After fixation, the cells were washed in PBS plus 0.1% Triton X-100. The coverslips were successively covered with rabbit anti-*Paramecium* axonemal tubulin (1:50) for 30 min, monoclonal mouse anti-α-tubulin (1:500; Amersham Chemical Co., Arlington Heights, IL) for 15 min, Texas Red-labeled goat anti-rabbit (1:50) for 30 min, fluorescein-labeled goat anti-mouse (1:50) for 15 min, followed each time by washes with PBS plus 0.1% Triton X-100. The coverslips were mounted in moewiol and observed with a Zeiss Axiophot microscope. Photographs were taken either on iso-400 Kodak films or on hypersensitized Kodak tec-Pan (2615) films (Kirschner and Schulze, 1986).

Sample Preparation for the Detection of Dynamic Microtubules by Confocal Immunofluorescence Microscopy and for Microtubule Length Measurements

We noticed that preextraction of the cells for 10 s is sufficient to cause some depolymerization at microtubule extremities (~1–2 μm). Therefore for length measurements and confocal microscopy, the cells were fixed according to the following procedure. After microinjection, the cells were washed for 2 s in PBS at 37°C and fixed for 10 min at room temperature in a solution of 0.3% glutaraldehyde prepared in the permeabilization buffer (80 mM K-Pipes pH 6.8, 5 mM EGTA, 1 mM $MgCl_2$, 0.5% Triton X-100). The cells were then washed in PBS for 10 s and placed for 7 min (twice) in PBS pH 8.0 containing 1 mg/ml $NaBH_4$. After this quenching step, the cells were further washed quickly in PBS and in PBS plus 0.1% Triton X-100. Immunolabeling was carried out with the rabbit anti-*Paramecium* axonemal tubulin (1:50) for 50 min. followed by the monoclonal anti-α + β tubulin (1:400), for 30 min. After two 5-min washes in PBS containing 0.1% Triton X-100, the coverslips were incubated with fluorescein-labeled goat anti-rabbit (1:100) and rhodamine-labeled goat anti-mouse (1:40 for 30 min each). After two 10-min washes in PBS containing 0.1% Triton X-100, the coverslips were post fixed for 30 min in a solution of 4% paraformaldehyde prepared in microtubule stabilizing buffer. The coverslips were then washed twice for 5 min in PBS and treated for 20 min with 100 mM NH_4Cl in PBS (pH 6.9). After a further two 5 min washes in PBS, the coverslips were mounted in 50% glycerol prepared in PBS containing 100 mg/ml 1,4 diazobicyclo-[2.2.2] octane (DABCO; Sigma Chemical GmBH, Deisenhofen, FRG) (Bacallao and Stelzer, 1989). Finally, the coverslips were sealed with nail polish.

Image Acquisition and Image Processing Using the Modular Confocal Microscope (MCM)

The MCM used in this work was developed and built at the European Molecular Biology Laboratory. An Argon-ion laser (Spectra-physics 2020-05) produced a line at 496 nm, which was used to excite both FITC and rhodamine. The filter sets used in the illumination path and in the detection path were nonstandard and therefore need some description. The dichroic mirror (DC1) that separates the excitation from the emission light was a DR 500 LP (Omega Opticals, Brattleboro, VT). The emission from both dyes was separated in the fluorescence MCM by a DR 560 LP (Omega Opticals). The transmitted light passed an OG 610 (Schott, Mainz, FRG) and gave the image of the rhodamine-labeled target while the deflected light passed a band-pass filter (530 DF 30) before it was detected in the FITC channel. Both channels were detected in parallel and the use of a single excitation line guaranteed a perfect overlap on a picture element (pixel) basis. Images were recorded by first selecting a reasonable sample with the conventional microscope, switching to the confocal mode, centering the sample, adjusting the field size and then generating an X/Z image through the nucleus. The X/Z image was used to determine the start and end positions in a series. The pitch along the Z-axis was always 0.4 μm. The number of averages (16 or 32) was selected such that the image in the rhodamine channel gave sufficient contrast to the human eye to observe individual microtubules.

The images all consisted of 512 lines/image and 512 pixels/line. Since the scanner of the MCM produces 900 lines per second, one image is recorded per channel every 0.6 s. Each image in a series is recorded with a 16-bit word per pixel but stored with 8 bits (1 byte) per pixel. The user may adjust only the gain of photomultipliers such that the brightest parts in the object are not over exposed in the image. The black level is not adjustable. Apart from averaging, no data processing was performed during the recording process.

The stereo pairs were calculated (Rosa et al., 1989) for each channel and then overlaid with the computer. The color green was given to FITC and

red to rhodamine. Overlaying could be done by using the brightest color, giving either a red or a green pixel (MCM), or by mixing red and green, resulting in red, green, and yellow pixels (View program). In both cases, brightness and contrast must be adjusted to suit the human eye. For the analysis of single microtubules, partial stereos and overlays were made using the MCM program. The analysis was performed on color stereo slides that were taken directly from a television monitor (Polaroid freeze frame) on Fujichrome 100 ASA film. For black and white overlays, the colors were transformed to white (FITC) and to grey (rhodamine) before being photographed on Kodak TMAX 100. Images that were processed using VIEW were converted to 24 bit-TIFF (Tagged Image File Format) images and sent to a Honeywell slide writer in which they were printed on color slides. The program VIEW, run on a microVAX station 3100, was kindly provided by the Lawrence Livermore Laboratories (Livermore, CA) and modified at the European Molecular Biology Laboratory.

Antibody-blocking Technique for Detection of Stable Microtubules

After injection of cells with *Paramecium* axonemal tubulin (4 or 2 mg/ml), cells were incubated at 37°C in a CO_2 incubator for 30 min, 1 h, and 2 h. The cells were then washed with PBS at 37°C for 2 s and fixed with glutaraldehyde or methanol as described above. We used the antibody-blocking procedure previously described for biotinylated tubulin by Schulze and Kirschner (1987). The dynamic network was stained with the rabbit anti-*Paramecium* axonemal tubulin followed by a series of four secondary antibodies. The microtubules which had not incorporated *Paramecium* tubulin (stable microtubules) were then revealed by the mouse antitubulin mAb. The rabbit anti-*Paramecium* tubulin (1:50) was applied for 1 h, followed by fluorescein-labeled goat anti-rabbit (40 min), fluorescein rabbit anti-goat (40 min), unlabeled goat anti-rabbit (40 min), and unlabeled rabbit anti-goat (40 min). These fluorescent and unlabeled secondary antibodies were used, respectively, at concentrations of 5 and 6 μg/ml. The mouse anti-α-tubulin mAb (1:1,000) was then applied for 20 min and revealed by a rhodamine-labeled rat anti-mouse (1:30; 20 min). Between each incubation the cells were washed five times and incubated for 10 min in PBS containing 0.1% Triton X-100. The coverslips were mounted in moewiol and observed in a Zeiss Axiophot microscope.

Length Measurements

Magnified pictures of microinjected cells were displayed on a television monitor using an RCA video camera (TC 10055/U). Microtubule segments (~300/cell) were measured using an IBAS (Carl Zeiss GmBH) image-processing system.

Results

Pattern of Tubulin Incorporation into Microtubules in Fibroblasts and MDCK Cells as Observed by Conventional Microscopy

We have determined the sites of incorporation of tubulin into microtubules in Vero and MDCK cells by injecting *Paramecium* axonemal tubulin. This is a good marker since it copolymerizes with mammalian tubulin and is specifically recognized by a polyclonal antibody (Geuens et al., 1989). We routinely injected the *Paramecium* axonemal tubulin solution at 1 mg/ml. In isolated fibroblastic cells (Vero, not shown) fixed a few minutes after injection, the *Paramecium* tubulin was incorporated into segments scattered throughout the cytoplasm. There was also a strong incorporation at the centrosome. A similar pattern of incorporation was observed in confluent Vero cells with a prominent incorporation at the centrosome (Fig. 1, *a* and *b*, *arrow*). This confirmed previous observations obtained after the injection of fluorescein-labeled tubulin (Soltys and Borisy, 1985) or biotinylated tubulin (Kirschner and Schulze, 1986). Visualization of microtubules by immunoelectron microscopy of thin sections showed that labeled and unlabeled microtubules were continuous with a sharp transition between unlabeled and labeled domains (Antony, C., data not shown, but see Geuens et al. (1989), and Kirschner and Schulze, (1986). The strong incorporation observed at the centrosome corresponded to new microtubules nucleated by the pericentriolar material.

In isolated MDCK cells, the pattern of *Paramecium* tubulin incorporation varied from cell to cell but it was mostly localized close to the nucleus and relatively focussed although not as much as in Vero cells (Fig. 1, *c* and *d*). The arrow and insert show the zone of increased nucleation. In most confluent MDCK cells, the region of increased incorporation was much more dispersed. Often, it did not even exist (Fig. 1, *e* and *f*). This suggested that after the establishment of cell contacts, the nucleating material was dispersed in the cytoplasm, making it impossible to distinguish newly nucleated microtubules from elongation at the end of preexisting microtubules. Alternatively, the establishment of cell junctions could have reduced the frequency of new nucleation events to such an extent that only the ends of microtubules were dynamic (complete suppression of dynamic instability in favor of tempered instability; see Sammak and Borisy, 1988). It was impossible to distinguish between these two possibilities by classical immunofluorescence microscopy. We first tried to track the newly assembled microtubules by immunogold EM. As expected, this proved to be a tremendous and hopeless task. We therefore decided to do an analysis of microtubule nucleation using the new confocal microscope (MCM) recently developed at the European Molecular Biology Laboratory.

Analysis of Microtubule Nucleation in Isolated and Confluent MDCK Cells by Confocal Microscopy

To show the existence of newly nucleated microtubules in MDCK cells, we had to find small microtubules containing mixed MDCK and *Paramecium* axonemal tubulin that were not at the end of an MDCK-only microtubule. This required spatial resolution in three dimensions and double immunofluorescence without spatial shift between the microtubules labeled with rhodamine and fluorescein. This was achieved by exciting both fluorochromes at the same wavelength (496 nm), separating the light emitted by each fluorochrome with appropriate filters and acquisition of both rhodamine and fluorescein signals simultaneously in the computer. Obviously, 496 nm was not the optimal wavelength to excite rhodamine. Therefore, the intensity of the rhodamine signal was slightly lower than that of the fluorescein signal and we choose to label the *Paramecium* tubulin with a fluorescein-tagged antibody. Fig. 2 shows a typical result. The colors are artificial. Red corresponds to MDCK tubulin and yellow-green to the mixture *Paramecium*-MDCK tubulin. In the isolated cell at the very edge of a cluster of cells shown in Fig. 2 *a*, most of the tubulin incorporation observed at the periphery of the cytoplasm corresponded to elongation of preexisting microtubules (*arrowheads*). Intense incorporation was found in an area of ~7 μm in diameter, close to the nucleus (*arrow*). In this region many microtubules were yellow and clearly not at the end of a red microtubule, indicating that they were newly nucleated. Most of these microtubules were short (1–2 μm) and careful examination revealed a yellow background of dots which were not found elsewhere in the cytoplasm. They probably corresponded to very early nucleation events. These newly nucleated microtubules were arranged in a radial pattern and

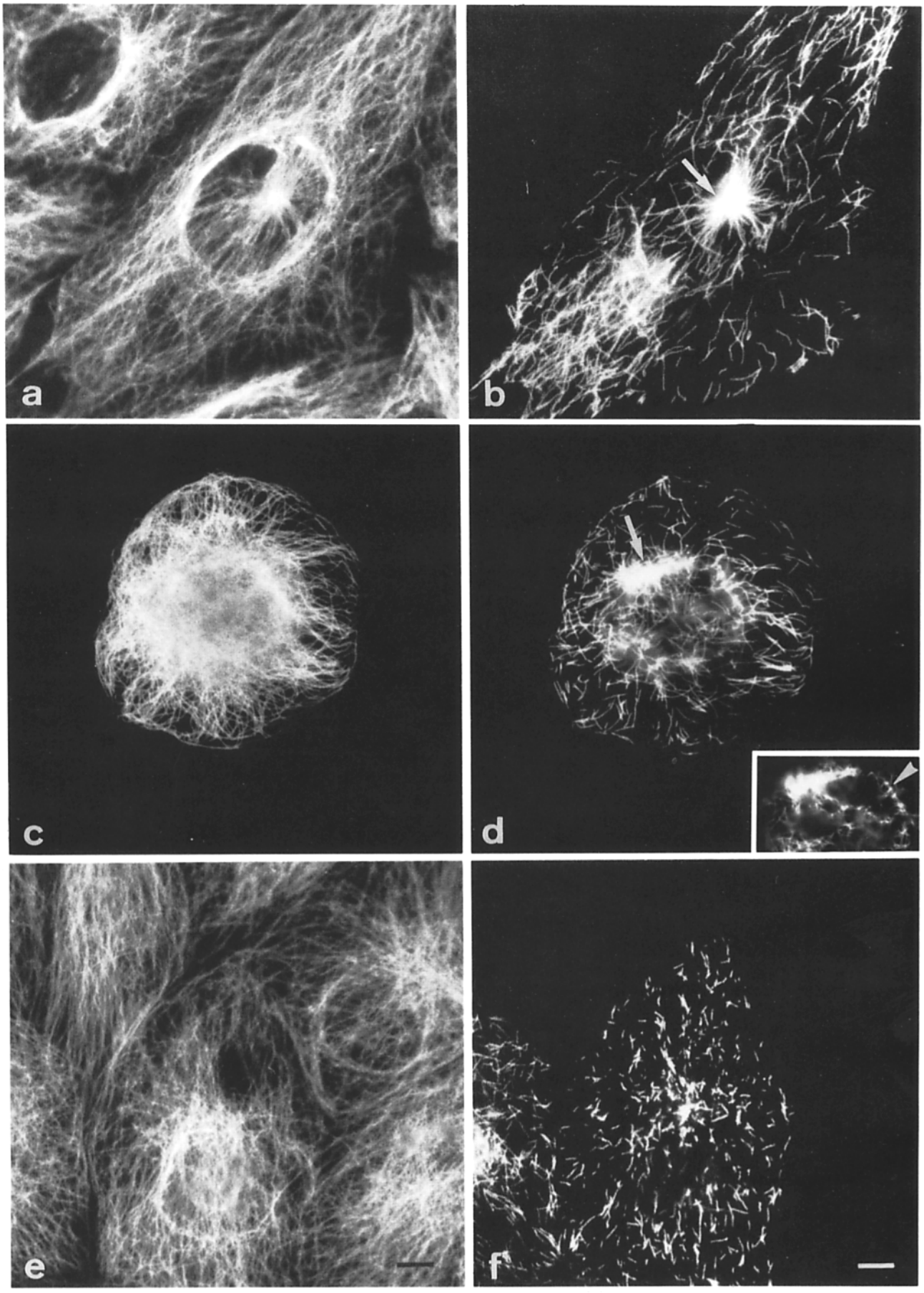
a
b
c
d
e
f

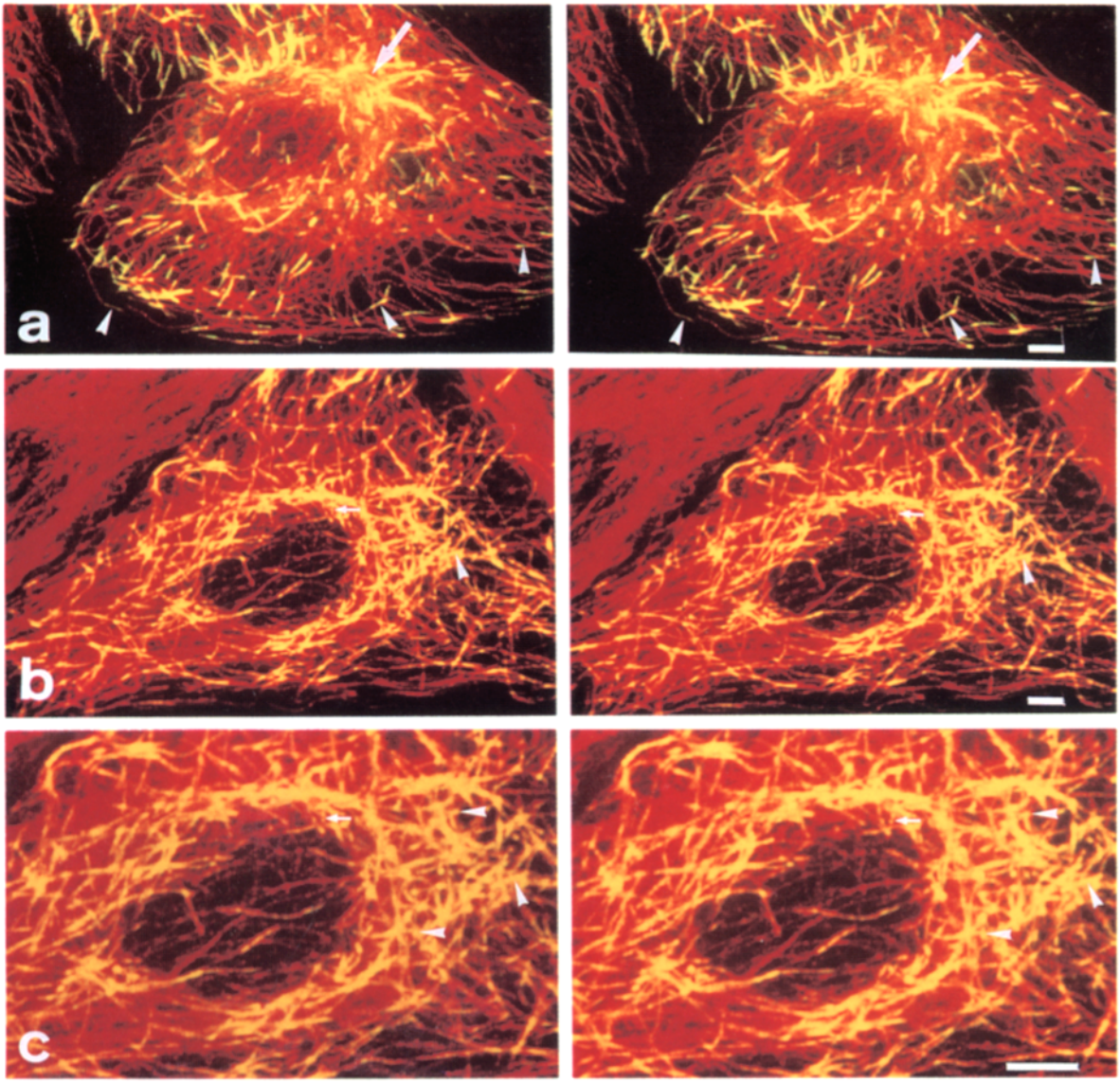

Figure 2. Confocal microscope stereo-pair images of overlaid total microtubules (*red*) and *Paramecium* tubulin (*yellow-green*) incorporated into the microtubules of MDCK cells. (*a*) Single cell. This cell was fixed about one min after injection. Note the region of intense incorporation next to the nucleus (*arrow*) and microtubule elongation (red microtubules followed by yellow-green microtubules) in the periphery of the cell (*arrowheads*). (*b*) Confluent cell. This cell was fixed ~2.0 min after injection. Arrowheads show newly nucleated microtubules. Arrow shows newly nucleated microtubules growing vertically along the nucleus. (*c*) Enlargement of the central region of the cell shown in *b*. Arrowheads show some newly nucleated microtubules. Arrow shows the two microtubules that grow along the nucleus. Bars: (*a–c*) 5 μm.

found in an ovoid region ~7 μm in diameter in the horizontal plane and ~1.6–2 μm in the vertical axis. The whole cell was recorded in 16 horizontal optical sections, 0.4 μm each. The area of intense nucleation was found in sections 7–10 (starting from the coverslip), that is approximately half-way between the base and top of the cell. This zone of nucleation probably contained the two centrioles that are together and close to the nucleus in isolated cells (Buendia et al., 1990).

Figure 1. Pattern of tubulin incorporation observed by conventional fluorescence microscopy. Fluorescein channel (*a*, *c*, and *e*): total microtubule network. Texas Red channel (*b*, *d*, and *f*): *Paramecium* tubulin. In confluent Vero cells (fibroblasts, *a* and *b*), *Paramecium* axonemal tubulin incorporates at microtubule ends and off the centrosome (*arrow*). In single MDCK cell (*c* and *d*), *Paramecium* tubulin incorporates into segments scattered in the cytoplasm and there is an area of increased incorporation around the nucleus (*arrow*); inset: focusing was made on the edge of the nucleus from which microtubules seemed to grow (*arrowhead*). In confluent MDCK cells (*e* and *f*), *Paramecium* tubulin incorporates into segments scattered in the cytoplasm, and there is no apparent region of increased incorporation. The cells were fixed with methanol at −20°C (*a* and *b*) 3 min, (*c* and *d*) 1 min, 17 s and (*e* and *f*) 1 min after injection of *Paramecium* axonemal tubulin and stained by double immunofluorescence as described in Materials and Methods. Bar, 5 μm.

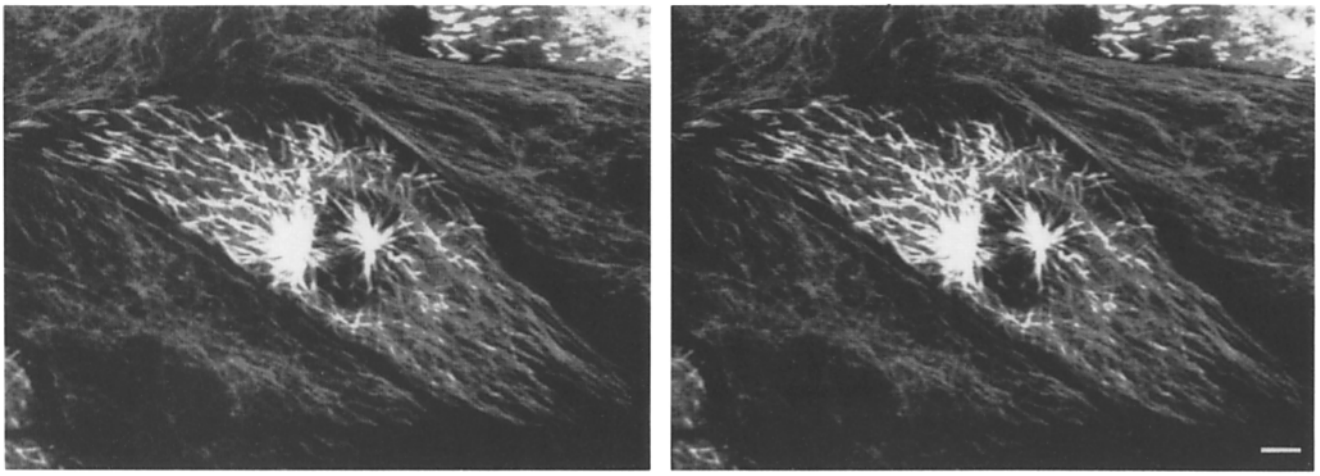

Figure 3. Confocal microscope stereo pair images of overlaid total microtubules (*gray*) and *Paramecium* axonemal tubulin (*white*) incorporated into the microtubules of a prophasic MDCK cell: there is a strong tubulin incorporation at the duplicated centrosomes. This cell was fixed ~1.5 min after injection. Bar, 5 μm.

The overall distribution of tubulin incorporation in a confluent cell is shown in Fig. 2, *b* and *c*. Here, newly nucleated microtubules (*arrowheads*) were found in a large region of the cytoplasm (~15 μm in diameter) on one side of the nucleus with microtubules growing in all directions. Some of them were also found to grow vertically along the nucleus (*arrow*). Two such microtubules are well visible in the enlargement in Fig. 2 *c*. They are clearly not at the end of a red microtubule towards the top of the cell. Examination of the same image from the bottom of the cell by inverting the two stereo images shows that they are not connected at the other end either (not shown).

The special patterns of tubulin incorporation observed in MDCK cells were not due to unknown artefacts occurring after injection of *Paramecium* tubulin. Indeed, the same tubulin injected in prophase MDCK cells was strongly incorporated at the centrosomes (Fig. 3). In this figure, the colors have been transformed to black and white (see Materials and Methods). White represents green (fluorescein-*Paramecium* tubulin); grey represents red (rhodamine-MDCK tubulin). This clearly shows that although the centrioles nucleate very few microtubules in MDCK cells during interphase, they become perfectly competent to nucleate in prophase, as in fibroblasts.

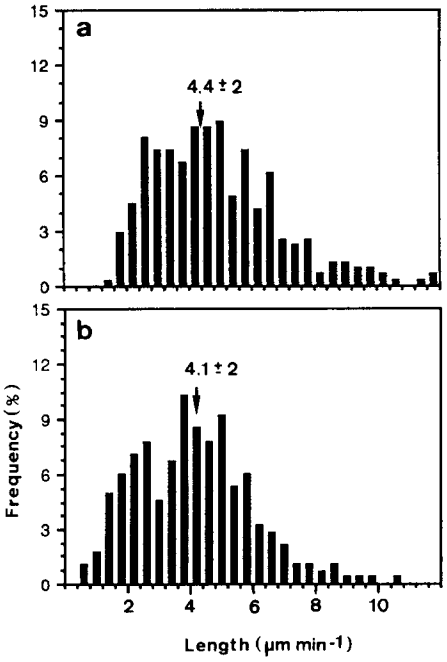

Figure 4. Histograms showing the distribution of microtubule elongation rate (microns/minute) in one isolated (*a*) and one confluent (*b*) MDCK cell, fixed (glutaraldehyde, no preextraction) respectively 29 and 52 s after injection.

The Elongation Rate of Individual Microtubules Is Similar in Isolated and Confluent MDCK Cells

The elongation rate was determined by measuring the length of microtubule segments containing *Paramecium* tubulin after various times of incorporation. This was done on images recorded by conventional fluorescence microscopy. The rate of incorporation was linear over 2 min of incorporation. Then, it became difficult to do the measurements because microtubules were too long. Fig. 4 shows the distribution of microtubule elongation rate in (*a*) individual and (*b*) confluent MDCK cells. Although the distribution pattern was slightly different, the mean elongation rate was very similar in isolated and confluent cells (~4 μm/min). This value is in agreement with values previously reported in fibroblast cells (Kirschner and Schulze, 1986). Microtubules elongate at rates that vary between 0.8 and 12 μm/min in a given cell. Similar results were obtained for 10 different isolated or confluent cells (3,000 length measurements). This high heterogeneity in elongation rate in a given cell is in agreement with previous findings where each microtubule seemed to display specific dynamic instability properties (Cassimeris et al., 1988; Sammak and Borisy, 1988; Sammak et al., 1987; Schulze and Kirschner, 1988).

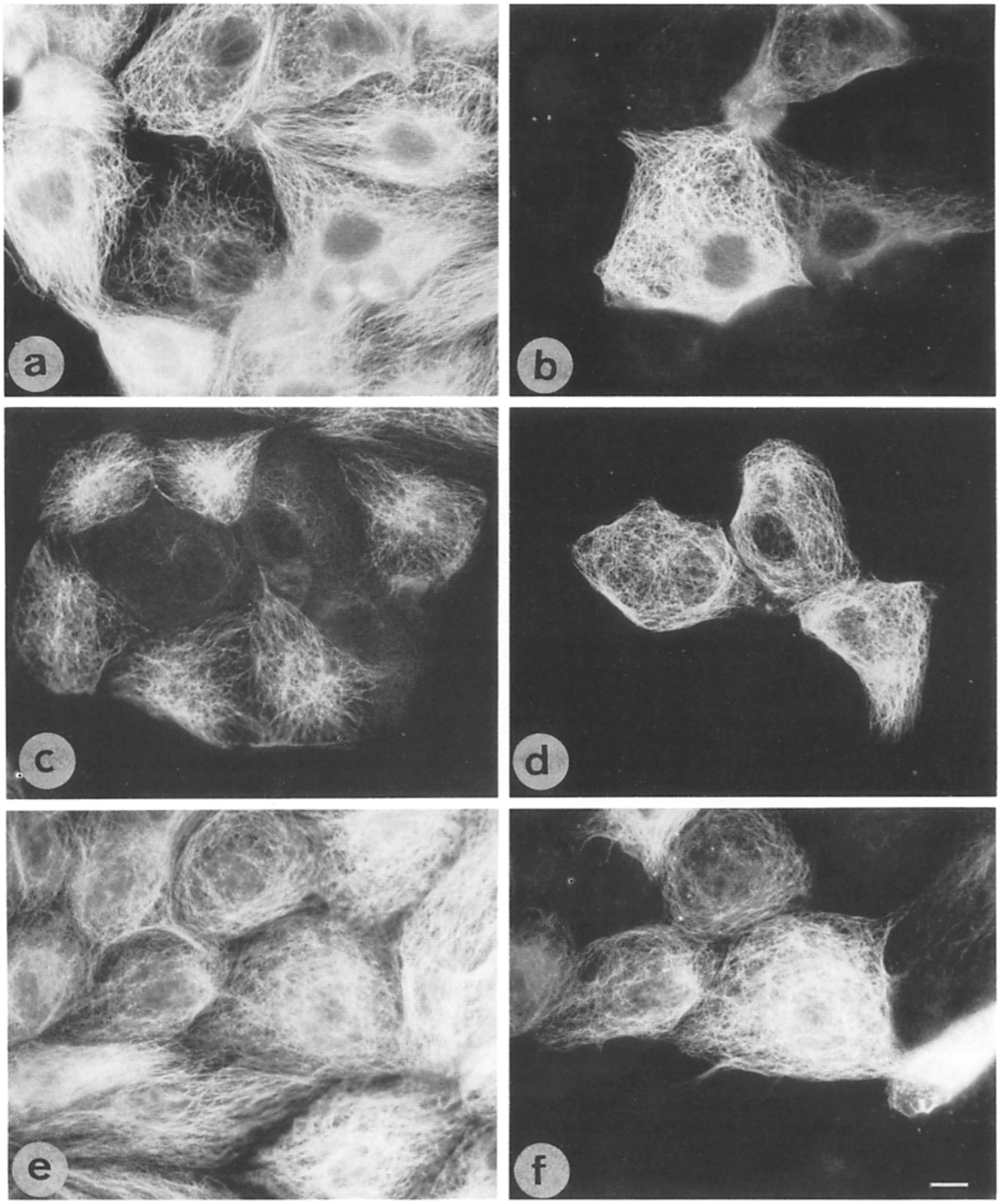

Figure 5. Microtubule stability is increased in confluent MDCK cells. Cells were fixed 30 min (*a* and *b*), 1 h (*c* and *d*), and 2 h (*e* and *f*), after injection of *Paramecium* tubulin. The cells were labeled with *Paramecium*-axonemal tubulin antibody (fluorescein channel) to show the dynamic microtubules (*b*, *d*, and *f*). After coating of these microtubules with several layers of secondary antibodies, microtubules that had not incorporated the *Paramecium* tubulin were detected by the antimammalian tubulin antibody (unblocked, stable microtubules, Texas red channel; *a*, *c*, and *e*). Bar, 10 μm.

Stable Microtubules in Isolated and Confluent Cells

To visualize stable microtubules, we applied the antibody-blocking technique developed by Schulze and Kirschner (1987) to our system. *Paramecium* tubulin was injected and the cells fixed after various times. The dynamic microtubules were labeled with the anti-*Paramecium* tubulin and coated with four more layers of secondary antibodies to prevent reaction to subsequent addition of antitubulin. The stable microtubules (that did not incorporate *Paramecium* tubulin) were not coated by the previous antibodies and could be visualized by a monoclonal antimammalian tubulin.

Table I. Frequency of Cells with Stable (S), Dynamic (D), and Uncertain (±) Microtubules

		% of cells with stable (S) and dynamic (D) microtubules	
		1 h	2 h
		%	
Isolated cells	T	(7)	(8)
	S	0	0
	D	100	100
	±	0	0
Cells in small clusters	T	(50)	(56)
	S	10	7.1
	D	90.0	92.9
	±	0.0	0.0
Confluent cells	T	(48)	(29)
	S	70.8	48.3
	D	16.6	27.6
	±	12.6	24.1

This was determined by the antibody-blocking technique, 1 and 2 h after microinjection of *Paramecium* ciliary tubulin. Stable microtubules are not blocked (detected by the antimammalian tubulin after blocking with the anti-*Paramecium* tubulin, see Fig. 5). *T*, total number of cells counted in each case.

In cells present in small clusters as well as at the edge of a subconfluent monolayer (Fig. 5, *a–d*) or in isolated cells (not shown), a minor network of curly microtubules was stable for ~30 min but not more (Table I). By contrast, in confluent cells, a large population of microtubules did not exchange subunits over a period of 2 h in ~50% of the cells (Fig. 5, *e* and *f*, and Table I). This shows that there is a coordinated change in the localization of microtubule nucleation events, microtubule stability, and microtubule organization after the establishment of cellular junctions in MDCK cells.

Discussion

Part of this study was made possible by the use of confocal microscopy. In fact, this investigation shows well both the resolution power and the limits of the method. Although we have been able to resolve individual microtubule nucleation events in relatively thick cells packed with endogenous microtubules, we have been unable to quantitate our data because it was impossible to identify all the events with certainty. This problem may be solved in the future by using an adequate program for computer analysis and redrawing of all events.

In this work, we have used MDCK cells grown on coverslips and not on filter supports. This was more convenient for the microinjection and in fact, the changes in microtubule organization between isolated and confluent cells are not very different when cells are grown on glass or on filter supports (one can compare the data of Bacallao et al., 1989 and Buendia et al., 1990). The main difference is that cells grown on glass coverslips do not reach a proper final polarization state. This has prevented us from studying microtubule dynamics in fully polarized cells. However, there are other difficulties to study this cell state because it is extremely difficult to microinject fully polarized cells grown on filters without damaging them.

The present investigation has shown three important points: (*a*) in isolated MDCK cells microtubules are not nucleated from the centrioles, but from a broad region localized close to the nucleus. The region of microtubule nucleation spreads out after the establishment of cell junctions just as microtubules lose their radial organization. This demonstrates previous speculations concerning the changes in microtubule nucleation following the establishment of cell contacts (Bacallao et al., 1989; Buendia et al., 1990). However, how microtubules are nucleated in MDCK cells still remains unclear. (*b*) Microtubule stability is increased in confluent cells as compared to single cells or cells in small clusters: a population of cells with microtubules remaining stable for >1 h appears in confluent cultures. This is in agreement with Pepperkok et al. (1990) and Wadsworth and McGrail (1990) who found two populations of microtubules in confluent MDCK cells, one of them having a $t_{1/2}$ of >72 min. (*c*) The elongation rate of individual microtubules is similar in isolated and confluent cells although microtubules are more stable in the latter. This suggests that the pool of soluble tubulin is not depleted in confluent cells. (In fact, at least 40% of the total tubulin is in soluble form in fully confluent cells; Buendia, B., unpublished and see Pepperkok et al., 1990.) This also suggests that in confluent cells many microtubules undergo tempered dynamic instability (Sammak and Borisy, 1988) rather than catastrophic dynamic instability (Mitchison and Kirschner, 1984) and that the establishment of cell contacts reduces the frequency of transitions between growing and shrinking microtubules (Pepperkok et al., 1990). Finally, we found frequent elongation events, even in confluent cells, suggesting that microtubule stabilization is not due to extensive plus end capping of microtubules in our conditions. We cannot rule out, however, that some microtubules were indeed capped at their plus end.

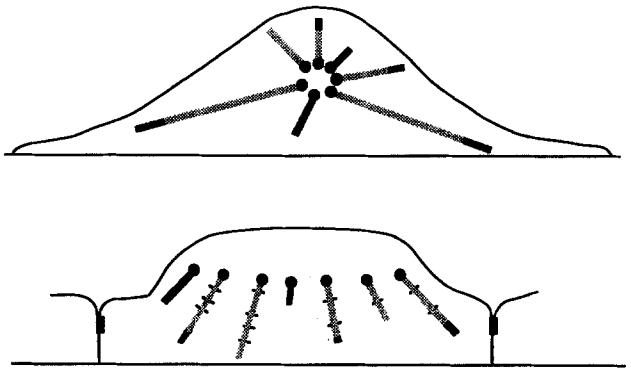

Figure 6. Possible mechanism of microtubule reorientation during the polarization of MDCK cells. (*top*) In isolated cells, 24 h after plating, newly nucleated microtubules are concentrated in an area near the cell center. Microtubules radiate in the cytoplasm and have a $t_{1/2}$ of <30 min. (*Bottom*) In confluent cells grown on glass, newly nucleated microtubules appear scattered in the cytoplasm, probably because the microtubule nucleating material spreads out and microtubule stability is increased.

This is obviously a very schematic outline of how microtubules may reorientate during polarization. It does not intend to be entirely exact but rather to help the reader. Microtubules are represented by shaded bars, growing microtubules by filled bars, stabilizing factors by dashes along microtubules, and nucleating material by black dots. Tight junctions are symbolized by fat lines between cells.

These results together with previous studies (Bacallao et al., 1989; Bré et al., 1987; Buendia et al., 1990), suggest that upon the establishment of cellular junctions, the microtubule-nucleating material, that is not tightly associated with centrioles in interphase, disperses. As a consequence, newly nucleated microtubules appear scattered (Fig. 6, *a* and *b*), several of them being arranged vertically along the sides of the nucleus. Microtubules are stabilized as the cells become more confluent (Fig. 6 *b*). It is possible that stabilizing factors are absent in cells lacking contacts. If this were the case, the establishment of junctions could increase their level either through increased synthesis or decreased degradation rate. Alternatively, the stabilizing factors may always be present but relocalized or their activity modified by slow posttranslational modifications in response to the assembly of cell junctions.

It has been hypothesized that microtubules could be rearranged in response to external signals by local stabilization through capping of their plus end (Kirschner and Mitchison, 1986; Kirschner and Schulze, 1986). Plus and minus end capping have been found in *Drosophila* wing epithelial cells (Mogensen et al., 1989). This was observed in finally polarized cells, in situ. In MDCK cells, the situation is less clear. As already mentioned, we always find a high number of microtubules that incorporate tubulin at their ends. This suggests that microtubules are first stabilized along their length, rather than being capped at their plus end. Whether some microtubules become capped at their plus ends during final polarization remains an open question. In any case, a picture emerges from our results suggesting that in epithelial cells, microtubule reorganization involves relocalization of microtubule nucleating material in the apical domain, concomitantly with microtubule stabilization. This reorganization may also involve actual movements of the stabilized microtubules (Pepperkok et al., 1990). Actin microfilaments are required for the separation of centrioles after the establishment of cell contacts (Buendia et al., 1990). It is likely that they play an important role in microtubule reorientation during the polarization process. The role of nucleation center relocalization in reorganization of the microtubule network during cell differentiation seems to be important in many other systems (Dylewsky and Keenan, 1984; Houliston et al., 1987; McNiven and Porter, 1988; Mogensen et al., 1989; Okabe and Hirokawa, 1988; Tassin et al., 1985*a*; Tucker et al., 1986; Zeligs, 1979). The challenge is now to find out how external signals control the positioning of this material as well as microtubule dynamics and movements.

We thank A. Adoutte (CNRS), B. Buendia, T. Kreis, and K. Simons (EMBL) for discussions and critical reading of the manuscript, P. Haenninen and C. Storz (EMBL) for efficient help with the use of the confocal microscope and computer programs as well as Y. Cully (EMBL) for his patience and expert help in photographic reproduction.

Received for publication 28 May 1990 and in revised form 18 September 1990.

References

Adoutte, A., M. Claisse, R. Maunoury, and J. Beisson. 1985. Tubulin evolution: ciliate-specific epitopes are conserved in the ciliary tubulin of metazoa. *J. Mol. Evol.* 22:220–229.

Baas, P. S., M. M. Black, and G. A. Banker. 1989. Changes in microtubule polarity orientation during the development of hyppocampal neurons in culture. *J. Cell Biol.* 109:3085–3094.

Bacallao, R., and E. H. K. Stelzer. 1989. Preservation of biological specimens for observation in a confocal fluorescence microscope and operational principles of confocal fluorescence microscopy. *Methods Cell Biol.* 31:437–452.

Bacallao, R., C. Antony, C. Dotti, E. Karsenti, E. H. K. Stelzer, and K. Simons. 1989. The subcellular organization of MDCK cells during the formation of a polarized epithelium. *J. Cell Biol.* 109:2817–2832.

Balcarova-Stander, J., S. E. Pfeiffer, S. D. Fuller, and K. Simons. 1984. Development of cell surface polarity in the epithelial Madin-Darby canine kidney (MDCK) cell line. *EMBO (Eur. Mol. Biol. Organ.) J.* 3:2687–2694.

Bré, M H., T. E. Kreis, and E. Karsenti. 1987. Control of microtubule nucleation and stability in Madin-Darby canine kidney cells: the occurrence of non centrosomal, stable detyrosinated microtubules. *J. Cell Biol.* 105:1283–1296.

Buendia, B., M. H. Bré, G. Griffiths, and E. Karsenti. 1990. Cytoskeletal control of centrioles movement during the establishment of polarity in MDCK cells. *J. Cell Biol.* 110:1123–1136.

Cassimeris, L., N. K. Pryer, and E. D. Salmon. 1988. Real time observations of microtubule dynamic instability in living cells. *J. Cell Biol.* 107:2223–2231.

Cohen, J., A. Adoutte, S. Grandchamp, L. M. Houdebine, and J. Beisson. 1982. Immunocytochemical study of microtubular structures throughout the cell cycle of Paramecium. *Biol. Cell.* 44:35–44.

Dylewsky, D. P., and T. W. Keenan. 1984. Centrioles in the mammary epithelium of the rat. *J. Cell Sci.* 72:185–193.

Geuens, G., A. M. Hill, N. Lavilliers, A. Adoutte, and M. De Brabander. 1989. Microtubule dynamics investigated by microinjection of Paramecium axonemal tubulin: lack of nucleation but proximal assembly of microtubules at the kinetochores during prometaphase. *J. Cell Biol.* 108:939–953.

Houliston, E., S. J. Pickering, and B. Maro. 1987. Redistribution of microtubules and pericentriolar material during the development of polarity in mouse blastomeres. *J. Cell Biol.* 104:1299–1308.

Inoué, S. 1981. Cell division and the mitotic spindle. *J. Cell Biol.* 81:131s–147s.

Kirschner, M., and T. Mitchison. 1986. Beyond self-assembly: from microtubules to morphogenesis. *Cell.* 45:329–342.

Kirschner, M., and E. Schulze. 1986. Morphogenesis and the control of morphogenesis in cells. *J. Cell Sci. Suppl.* 5:293–310.

Kreis, T. E. 1986. Microinjected antibodies against the cytoplasmic domain of vesicular stomatitis virus glycoprotein block its transport to the cell surface. *EMBO (Eur. Mol. Biol. Organ.) J.* 5:931–941.

Kreis, T. E., V. J. Allan, R. Matteoni, and W. C. Ho. 1988. Interaction of elements of the Golgi apparatus with microtubules. *Protoplasma (Berl.).* 145:153–159.

McNiven, M. A., and K. R. Porter. 1988. Organization of microtubules in centrosome-free cytoplasm. *J. Cell Biol.* 106:1593–1605.

Mitchison, T., and M. Kirschner. 1984. Dynamic instability of microtubule growth. *Nature (Lond.).* 312:237–242.

Mogensen, M. M., J. B. Tucker, and H. Stebbings. 1989. Microtubule polarities indicate that nucleation and capture of microtubules occurs at cell surfaces in *Drosophila*. *J. Cell Biol.* 108:1445–1452.

Okabe, S., and N. Hirokawa. 1988. Microtubule dynamics in nerve cells: analysis using microinjection of biotinylated tubulin into PC12 cells. *J. Cell Biol.* 107:651–664.

Pepperkok, R., C. Schneider, L. Philipson, and W. Ansorge. 1988. Single cell assay with an automated capillary microinjection system. *Exp. Cell Res.* 178:369–376.

Pepperkok, R., M. H. Bré, J. Davoust, and T. E. Kreis. 1990. Microtubules are stabilized in confluent epithelial cells but not in fibroblasts. *J. Cell Biol.* 111:3003–3012.

Rosa, P., U. Weiss, R. Pepperkok, W. Ansorge, C. Niehrs, E. H. K. Stelzer, and W. Huttner. 1989. An antibody against secretogranin I (chromogranin B) is packaged into secretory granules. *J. Cell Biol.* 109:17–34.

Sammak, P. J., and G. G. Borisy. 1988. Direct observation of microtubule dynamics in living cells. *Nature (Lond.).* 332:724–726.

Sammak, P. J., G. J. Gorbsky, and G. G. Borisy. 1987. Microtubules dynamics in vivo: a test of mechanisms of turnover. *J. Cell Biol.* 104:395–405.

Schulze, E., and M. Kirschner. 1987. Dynamics and stable populations of microtubules in cells. *J. Cell Biol.* 104:277–288.

Schulze, E., and M. Kirschner. 1988. New features of microtubule behaviour. *Nature (Lond.).* 334:356–359.

Soltys, E. J., and G. G. Borisy. 1985. Polymerization of tubulin in vivo: direct evidence for assembly onto microtubule ends from centrosomes. *J. Cell Biol.* 100:1682–1689.

Tassin, A. M., B. Maro, and M. Bornens. 1985*a*. Fate of microtubule organizing centers during in vitro myogenesis. *J. Cell Biol.* 100:35–46.

Tassin, A. M., M. Paintrand, E. G. Berger, and M. Bornens. 1985*b*. The Golgi apparatus remains associated with microtubule organizing centers during myogenesis. *J. Cell Biol.* 101:630–638.

Thyberg, J., and S. Moskalewski. 1985. Microtubules and the organization of the Golgi complex. *Exp. Cell Res.* 159:1–16.

Tucker, J. B., M. J. Milner, D. A. Currie, J. W. Muir, D. A. Forrest, and M. J. Spencer. 1986. Centrosomal microtubule organizing centers and a switch in the control of protofilament number for cell surface-associated microtubules during Drosophila wing morphogenesis. *Eur. J. Cell Biol.* 41:279–289.

Vale, R. D. 1987. Intracellular transport using microtubules-based motors. *Annu. Rev. Cell Biol.* 3:347–378.

Wadsworth, P., and M. McGrail. 1990. Interphase microtubule dynamics are cell type specific. *J. Cell Sci.* 95:23–32.

Zeligs, J. D. 1979. Association of centrioles with clusters of apical vesicles in mitotic thyroid epithelial cells. Are centrioles involved in directing secretions? *Cell Tissue Res.* 201:11–21.